Journal of Maps

ISSN: (Print) (Online) Journal homepage: https://www.tandfonline.com/loi/tjom20

Analysis of the paraglacial landscape in the Ny-Ålesund area and Blomstrandøya (Kongsfjorden, Svalbard, Norway)

Ivar Berthling , Claudio Berti , Vania Mancinelli , Laura Stendardi , Tommaso Piacentini & Enrico Miccadei

To cite this article: Ivar Berthling , Claudio Berti , Vania Mancinelli , Laura Stendardi , Tommaso Piacentini & Enrico Miccadei (2020) Analysis of the paraglacial landscape in the Ny-Ålesund area and Blomstrandøya (Kongsfjorden, Svalbard, Norway), Journal of Maps, 16:2, 818-833, DOI: 10.1080/17445647.2020.1837684

To link to this article: https://doi.org/10.1080/17445647.2020.1837684

JOURNAL OF MAPS
2020, VOL. 16, NO. 2, 818–833
https://doi.org/10.1080/17445647.2020.1837684

Analysis of the paraglacial landscape in the Ny-Ålesund area and Blomstrandøya (Kongsfjorden, Svalbard, Norway)

Ivar Berthling [a]*, Claudio Berti [b], Vania Mancinelli [c], Laura Stendardi [d], Tommaso Piacentini [c] and Enrico Miccadei [c]

[a]Department of Geography, NTNU-Norwegian University of Science and Technology, Trondheim, Norway; [b]Idaho Geological Survey, University of Idaho, Moscow, ID, USA; [c]Department of Engineering and Geology, Laboratory of Tectonic Geomorphology and GIS, Università degli Studi "G. D'Annunzio" Chieti-Pescara, Chieti Scalo (CH), Italy; [d]Institute for Earth Observation, Eurac Research, Bolzano, Italy

ABSTRACT

Ice cover changes have affected the Svalbard Islands during the Quaternary and conditioned a complex paraglacial landscape. In these remote and poorly vegetated arctic areas, the integration of field investigations and analysis of aerial images and DTMs or terrestrial laser scanning, is effective in the understanding landscape features and changes. In this work, we present the results of a geomorphological investigation and mapping in two sites along the Kongsfjorden in NW Svalbard (Ny-Ålesund and Blomstrandøya). A specific analysis focused on the slope landforms along the rock slopes. The study is based on fieldwork that defined deposits and landforms distribution of areas with different bedrock and geomorphological context. The analysis of the rock slopes focused on weathering and erosion processes, estimating erosion rates of 0.15–0.37 mm/yr over the Holocene, consistent with other areas around the Kongsfjorden and close to the highest values found in arctic areas.

ARTICLE HISTORY
Received 12 May 2020
Revised 12 October 2020
Accepted 13 October 2020

KEYWORDS
Geomorphological map; surficial deposits; rock slopes; erosion rates; Kongsfjorden area; Spitsbergen

1. Introduction

High latitude environments are highly sensitive to climatic fluctuations, capable of inducing rapid changes both to ecosystems and distribution of geomorphological processes and landforms. Since the Last Glacial Maximum (LGM), massive changes in arctic environments are related to stages of ice retreat and advancement. As glaciers retreat, new landscapes are affected by rapid modifications, high erosion rates and sedimentation processes and by a transition to paraglacial environments, which incorporate all non-glacial earth surface processes, sediments, and landforms directly conditioned by glaciation and deglaciation (Ballantyne 2002; Church and Ryder 1972; Oliva et al. 2019; Slaymaker 2009, 2011 Strzelecki et al. 2020 and references therein).

The Svalbard Islands are located in the Arctic Sea at very high latitude (74–81°N) and presently have coverage of around 60% by ice caps and valley/fjord glaciers (Hagen et al. 1993). Since the LGM and more recently after the LIA (Little Ice Age), the glaciers have retreated to a large degree from the fjords and lowland areas, and paraglacial conditions have rapidly expanded. This process is well investigated in the Kongsfjorden area in NW Svalbard (e.g. Bourriquen et al. 2018; Forman et al. 2004; Gjermundsen et al. 2013; Hormes, Gjermundsen, and Rasmussen 2013; Lehmann and Forman 1992; Mercier and Laffly 2005). The variety of surface processes and landforms in this area has prompted studies on a wide range of geomorphological issues, including glacial features and deglaciation history, periglacial features, slopes, fluvial geomorphology and coasts (e.g. André 1997, 2009; Berthling and Etzelmüller 2007; Bernard et al. 2018; Bourriquen et al. 2018; Etienne, Mercier, and Voldoire 2008; Etzelmüller, Ødegard, and Sollid 2003; Hallet and Prestrud 1986; Henriksen et al. 2014; Kääb, Ramuntcho Girod, and Berthling 2014; Laffly and Mercier 2002; Mercier et al. 2009; Moreau et al. 2008). The permafrost features and active layer around 1–2 m and recent (last decade) measurements show a zero-amplitude depth of 5.5 m and a mean temperature of 2.8°C (rising over the last decade, Humlum, Instanes, and Sollid 2003; Boike et al., 2018). However, while geomorphological mapping was carried out in several specific sites in Svalbard (e.g. Evans et al. 2012; Pekala 2004; Rubensdotter et al. 2015; Rubensdotter, Larsen, and Lyså 2016; Sessford and Hormes 2013; Tolgensbakk, Sørbel, and Høgvard 2001), a detailed geomorphological map of the Kongsfjorden area is lacking (only two maps from 1960–1980 were published for the NW Brøgger-alvøya area; Joly 1969; Tolgensbakk and Sollid 1987).

CONTACT Enrico Miccadei enrico.miccadei@unich.it Department of Engineering and Geology, Laboratory of Tectonic Geomorphology and GIS, Università degli Studi "G. D'Annunzio" Chieti-Pescara, Via dei Vestini 31–66100, Chieti Scalo (CH), Italy
*Present address Research Council of Norway, Drammensveien 288, 0283 Oslo.

Therefore, the main aim of this work is the development of geomorphological maps describing the distribution of deposits and landforms in the paraglacial environment of the central area of Kongsfjorden, Svalbard. A specific investigation focused on (1) slope processes and (2) fan landforms affecting the rock slopes of the areas of Ny-Ålesund (N slope of Zeppelinfjellet) and Blomstrandøya (N slope of Bratliekollen). The areas were chosen as they include different morphological (rugged mountain areas and smoothed reliefs), geological (heterogeneous sedimentary sequences and sandy-calcareous metasediments) and glacial features (recently post LIA deglaciated areas and ancient post-LGM deglaciated areas). This study was based on integrated field investigation, remote data and observations, and geomorphological mapping. It is the result of a project on the geomorphological effects of glaciers' retreat on sensitive high latitudes and mountains geomorphological environments (Hols Project, RIS 5842; Slopes project, RiS 10150, http://www.researchinsvalbard.no/).

2. Study area

The Svalbard archipelago is located in the Arctic Ocean, about midway from Norway to the North Pole. Spitsbergen, the main island, features a rugged mountain landscape (highest peak, Newtontoppen, 1717m a.s.l.) and large ice fields and glacially eroded fjord systems. The study areas are located in Kongsfjorden (NW Spitsbergen, between 78°58' N, 11°23' E and 79°4' N, 11°38' E; Figure 1) and are respectively Ny-Ålesund, on the SW coast of Kongsfjorden, and Blomstrandøya, in the central part of the fjord near the NE coast.

In a geological perspective, the Kongsfjorden is located on the northern termination of the NNW-SSE Cenozoic fold and thrust belt of W Spitsbergen and along a NW-SE strike-slip fault zone (Bergh, Maher, and Braathen 2000; Cianfarra and Salvini 2015, 2016; Hjelle 1993; Leever et al. 2011). Three main bedrock domains characterise the area: (1) pre-Devonian metasediments and igneous rocks (northern side of Kongsfjorden and Blomstrandøya); (2) scattered Devonian sediments (red conglomerates and sandstones) tectonically interbedded into pre-Devonian metasediments (marble, Blomstrandøya island); and (3) Late Paleozoic to Early Triassic sedimentary sequences (i.e. carbonates, conglomerates and calcareous sandstones, Brøggerhalvøya), overlain by Paleocene coal-rich sediments (Hjelle et al. 1999). The bedrock sequences are covered by Quaternary continental and coastal unconsolidated deposits (e.g. till and diamicton, slope, fluvial and beach deposits).

Ny-Ålesund is situated on the Brøggeralvøya peninsula on the SW shore of Kongsfjorden (Figure 1). It is placed on an undulating plateau (at 10–50 m a.s.l.) bounded by steep rock slopes of high relief mountains (Zeppelinfjellet, 556 m a.s.l.; Berteltoppen, 785 m a.s.l.; Scheteligfjellet, 719 m a.s.l.) and by broad valleys of the main terrestrial glaciers (Austre-Vestre Brøggerbreen, Vestre Lovénbreen, Midtre Lovénbreen). The geological setting consists of Middle Carboniferous-Early Triassic sedimentary bedrock. The bedrock includes conglomerate, sandstone and shale with limestone, dolomite, and marl sequences (Gipsdalen Group), passing to shale, chert, limestone, and sandstone sequences (Templefjorden Group) and to sandstone and shale sequences (Sassendalen Group). These sequences are overlain by Paleocene sandstone, shales, conglomerates, coal-rich (Ny-Ålesund supergroup, Hjelle et al. 1999). The bedrock sequences are involved in NE-verging low-angle thrust fault and displaced by N-S and NNE-SSW high angle faults, with closely spaced joints and fractures systems (Cianfarra and Salvini 2015, 2016).

The Blomstrandøya island is in the middle of Kongsfjorden, in front of Ny-Ålesund and along the NW coast close to the Blomstrandbreen glacier, which until 1992 connected the island to the coast (Burton et al. 2016; Hagen et al. 1993; Svendsen et al. 2002; Sund and Eiken 2010; Figure 1). The island is ~5 km long and up to >4 km wide (~16.4 km^2), with maximum elevations at Bratliekollen (370 m a.s.l.) and Irgensfjellet (385 m a.s.l.). The geological setting consists of medium to high-grade metamorphic marble (Proterozoic age, Generalfjella Formation; Hjelle et al. 1999), largely covered by a thin cover of weathered bedrock. Scattered remnants of unmetamorphosed redbeds (Devonian) are present. The tectonic and metamorphic structures feature a N-S general trend. Two syn-metamorphic phases of isoclinal folding are followed by post-metamorphic crenulation and kink-folds associated with west-verging thrusts (Hjelle et al. 1999; Thiedig and Manby 1992).

Kongsfjorden shows an overall U-shape, with longitudinal and transversal undulations, strandflats, and tributary glacial valleys. During the Late Pleistocene, the glaciers covered the entire Kongsfjorden (Hormes, Gjermundsen, and Rasmussen 2013; Lehmann and Forman 1992; Svendsen et al. 2002 and references therein). After the LGM, climate amelioration induced glacier retreat, which led to an ice-free Kongsfjorden since 11–14 kyrs (Henriksen et al. 2014). The maximum middle Holocene to present ice advancement occurred during the Little Ice Age (1800s, early 1900s) (Burton et al. 2016; Lehmann and Forman 1992; Svendsen et al. 2002 and references therein). The surrounding landscape is characterised by contrasting alpine reliefs and strandflats. The mountainous areas feature large rock slopes, covered by talus slopes and cones. The glacial valleys incorporate systems of moraine ridges (for moraine

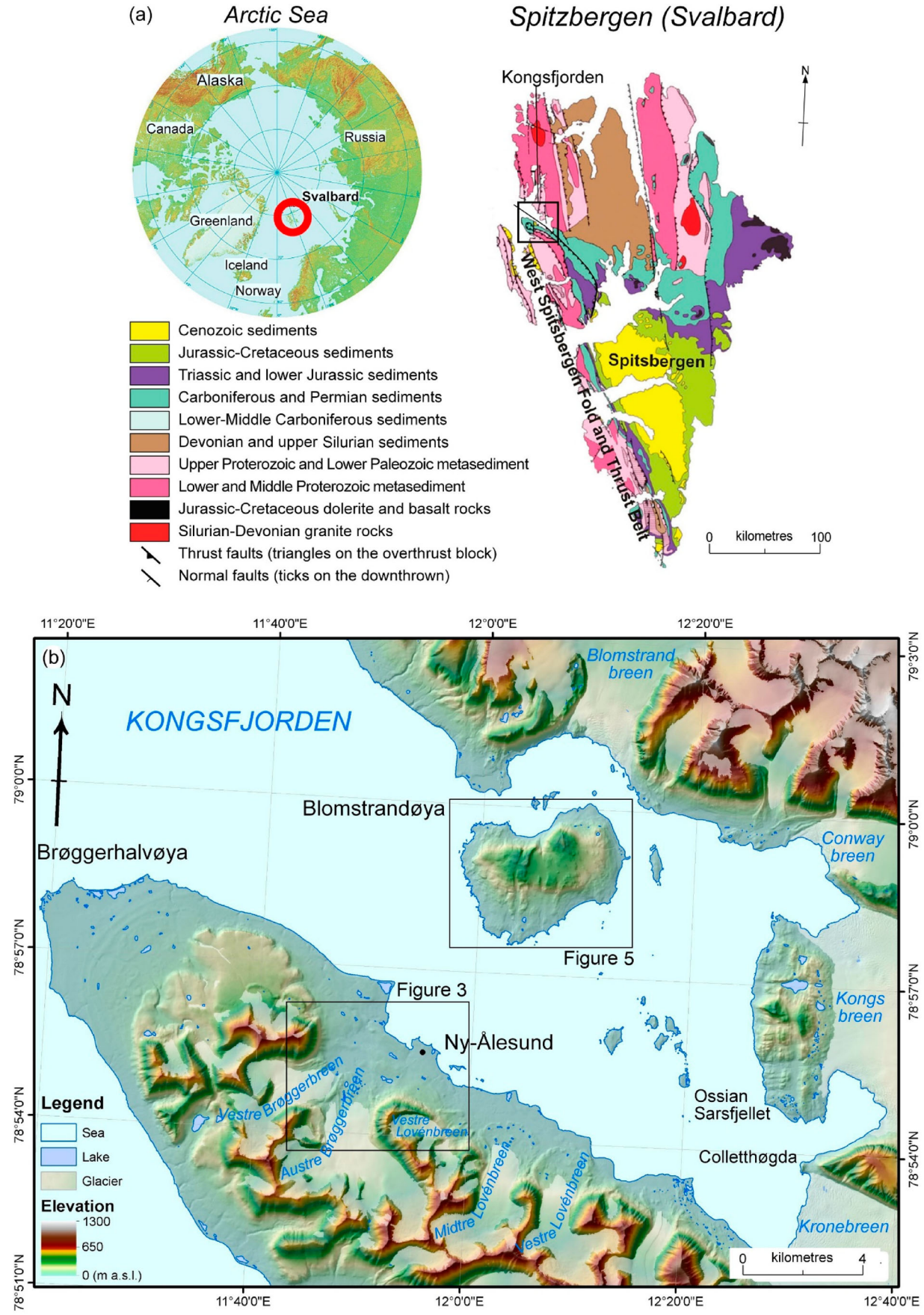

Figure 1. (a) Location map and geological scheme of Spitzbergen (Svalbard, Norway) (modified from Hjelle 1993). (b) Location map of the study areas (black boxes) in the Kongsfjorden (Svalbard, Norway); base data from Norwegian Polan Institute (https://geodata.npolar.no/).

terminology see Schomacker 2011). At the front of the terrestrial glaciers, streams breach through the moraines and outwash deposits develop large braided channel systems. The coastal areas are characterised by strandflats, sometimes bounded by a sharp transition to backing mountains as well as low coastal cliffs and linear or pocket beaches towards the sea. Raised beaches, whose genesis is related to post-glacial isostatic rebound, are preserved on the strandflats above the coastal cliffs (e.g. Bourriquen et al. 2018; Burton et al. 2016; Forman, Mann, and Miller 1987; Hallet 2013; Hallet and Prestrud 1986; Kääb, Ramuntcho Girod, and Berthling 2014; Mercier et al. 2009; Miccadei, Piacentini, and Berti 2016; Streuff 2013).

3. Methods

Geomorphological mapping carried out in this work integrated field and remote data resulting from (a) geomorphological fieldwork, (b) interpretation of orthophotos, Terrestrial Laser Scanner (TLS) data, Digital Surface Models (DSMs)and Digital Terrain Models (DTMs), and (c) DTMs processing and GIS mapping.

The geomorphological fieldwork was carried out in the summers of 2014 (Blomstrandøya, Hols Project, RIS 5842; Miccadei, Piacentini, and Berti 2016) and 2017 (Ny-Ålesund area, Slopes project, RIS 10150, http://www.researchinsvalbard.no/) with the support of the CNR Polarnet and Dirigibile Italia Station and according to Svalbard, Ny-Ålesund, and reserve areas regulations and requirements. The field investigations were focused on the mapping of surficial deposits and landforms at 1:5000 scale and were then reduced to 1:15,000–001:16,500 for mapping purposes. More detailed investigations analysed the relationship between rock slopes (i.e. Zeppelinfjellet and Bratliekollen), related deposits (forming fan-shaped landforms and talus slopes), and strandflats.

Fieldwork was supported by the acquisition of remotely sensed data (orthophotos taken in 1998, 2008, 2015) and a 5m-DTM (Table 1). Terrestrial laser scanning and UAV images (through SfM process) were used to realise DSMs and high-resolution orthophoto (Table 1). The interpretation of the orthophotos, and DTM-DSMs, by comparison of field and remote observations and 3D perspective, allowed: (1) interpolation of the field data and definition of the actual extent and perimeter of the main deposits and landforms observed; (2) mapping of the extent of fan-shaped landforms and talus slopes and specific sediment source areas; and (3) the geometrical infer of the average thickness of the fan-shaped landform (Figure 2). This approach is particularly effective in a cold bare environment, where the lack of vegetation cover leaves the deposits and landforms exposed.

GIS processing and geomorphological mapping was based on DTM-DSMs (Table 1) and has led to (1) the outline of the overall orographic setting of the Ny-Ålesund and Blomstrandøya areas; (2) the geomorphological maps of the two areas integrating field and remote-sensed data; and (3) the morphometric investigation of the fan-shaped landforms on the rock slopes of Zeppelinfjellet and Bratliekollen. In total, 49 landforms were analysed in Zeppelinfjellet and 24 in Bratliekollen. For each one, the perimeter was mapped from in-field surveys and aerial-terrestrial image analysis. The surface extent was calculated through GIS processing, and the maximum thickness was estimated from geometrical infer (Figure 2) combining field investigation and DTM-DSMs analysis. The volume was estimated for each landform and the sediment volume considering porosity (~25%) and ice content of the rock glaciers (~50%). Finally, the perimeter and the surface area of the source area or catchment of each landform were mapped and calculated.

Table 1. Images and terrain-surface models used in this work and related sources.

Data	Year	Resolution (m)	Aprox. error (m)	Area	Source
Orthophoto	1998	1	~1–2	Ny-Ålesund	Norwegian Polar Data https://geodata.npolar.no/
Orthophoto	2008	0.16	~0.5	Ny-Ålesund and Blomstrandøya	Norwegian Polar Data https://geodata.npolar.no/
Orthophoto	2015	0.30	~1	Ny-Ålesund and Blomstrandøya	Esri, Maxar, Earthstar Geographics (2015)
DTM	2009	5	~5	Ny-Ålesund	Norwegian Polar Data https://geodata.npolar.no/
DTM	2010	5	~5	Blomstrandøya	Norwegian Polar Data https://geodata.npolar.no/
DSM	2016	0.2	~0.5–1	Ny-Ålesund	UAV and SfM (process Agisoft Photoscan) Slopes Project, RiS 10150
Orthophoto	2016	0.2	~0.5–1	Ny-Ålesund	UAV and SfM (process Agisoft Photoscan) Slopes Project, RiS 10150
TLS Terrestrial laser scanner	2016	0.2	~0.1–0.5	Ny-Ålesund	Slopes Project, RiS 10150

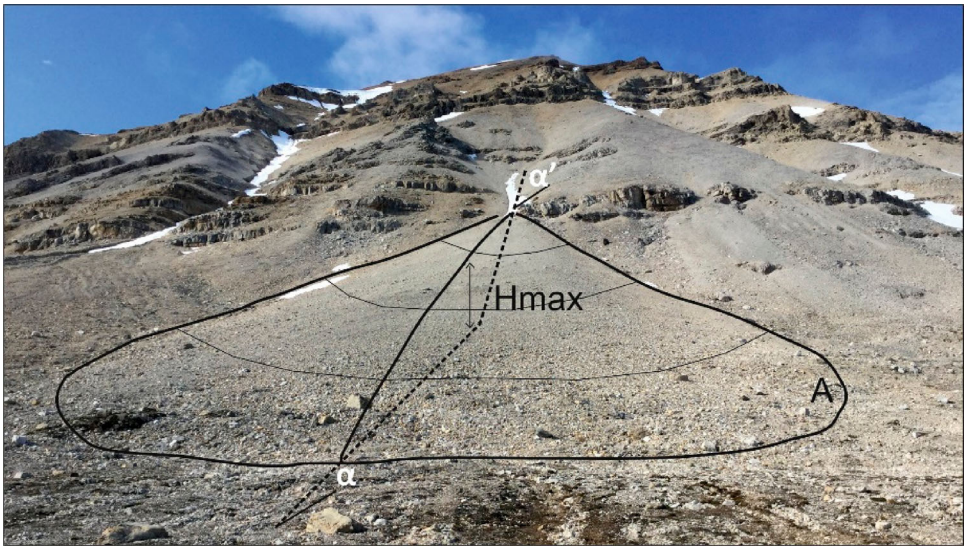

Figure 2. Geometrical calculation of the fan-shaped landforms thickness. H max: max thickness; α: slope angle of the lower part of the slope; α': slope angle of the upper rock slope.

4. Results

4.1. Geomorphological map of the Ny-Ålesund area

In the Ny- Ålesund area, the ridges orientations are from NW-SE (Lundryggen) to E-W (Zeppelinfjellet) to SW-NE (Berteltoppen) with rock slopes up to >45°, with subvertical rock cliffs (Figure 3). The valley bottoms and the strandflats have a low relief (<10°), with localised steep scarps (i.e. rock scarps, river valley scarps, moraine ridges). The present coast alternates rocky cliffs and gravel beaches (linear and pocket), including deltas and lagoons.

The Ny-Ålesund area is characterised by an extensive cover of surficial continental deposits (Figure 4) consisting of till and diamicton, slope (talus and rockfalls), fluvial, and beach deposits. Their thickness varies from a few metres (on the strandflats) to some tens of metres (at the base of the slopes and in the glacial valleys).

The recent (i.e. post-LIA) till and diamicton deposits (Figure 4a,b, see descriptions in the main map) form the terminal and lateral moraines of the present glaciers and cover the glacial valleys. Till and diamicton deposits from the post-LGM deglaciation were heavily reworked by periglacial and fluvial processes, particularly in the strandflat area (Figure 4c), and this makes them difficult to discern (in the map the main areas are defined). The flanks of the main ridges feature large talus slope and cone deposits, and occasionally rockfalls. The front of the main glaciers is characterised by rivers and outwash plains (i.e. Bayelva, Wexelva, Figure 4a,f,g) with alluvial sediments and large braided channels. The thickness of these deposits varies from <1 m in the small channels to up to >10 m in the main alluvial plains (derived from geomorphological interpretation). The coast is rimmed by discontinuous gravel beach deposits (Figure 4 h).

Glacial and slope landforms dominate the Ny-Ålesund area on the SW mountainous area and in the main valleys. The NE sector (i.e. strandflat) is mostly dominated by periglacial, fluvial, and coastal features overprinting older glacial landforms. In the main valleys (at the termination of the Austre and Vestre Brøggerbreen, Vestre and Midtre Lovénbreen glaciers), the extensive cover of till and diamicton deposits are arranged in an extensive system of lateral, medial, and terminal moraine ridges (Figure 4a,b). Terrestrial glaciers have been retreating since the LIA (Burton et al. 2016; Svendsen et al. 2002 and references therein) and different recessional moraines (according to Schomacker 2011), hosting several glacial lakes, are related to the rapid glacier retreat that has occurred over the last few decades. The mapping of glacier extent in 1998, 2008, and 2015 (from different sets of orthophotos) outlined an average retreat rate of ~30 m/yr from, for a total 500–550 m of frontal retreat from 1998 to 2015 in Austre and Vestre Brøggerbreen (calculated from the area of the deglaciated area divided by the glacier front width and by the number of years of the calculation). In the strandflat, the glacial landforms are almost entirely covered by fluvial deposits and periglacial landforms (i.e. patterned grounds, Figure 4c).

Slope landforms dominate the rock slopes (i.e. rock falls and talus slopes and cones; Figure 4d,e). Fluvial landforms characterise the outwash plains of the main glaciers, where the main rivers have formed large sandy-gravelly braided channels (Figure 4g). In the coastal area, rivers incise the bedrock, forming steep scarps and bedrock channels perpendicular to the coast (Figure 4f). The coast is characterised by alternating gravel beaches (up to 100 m wide, on the

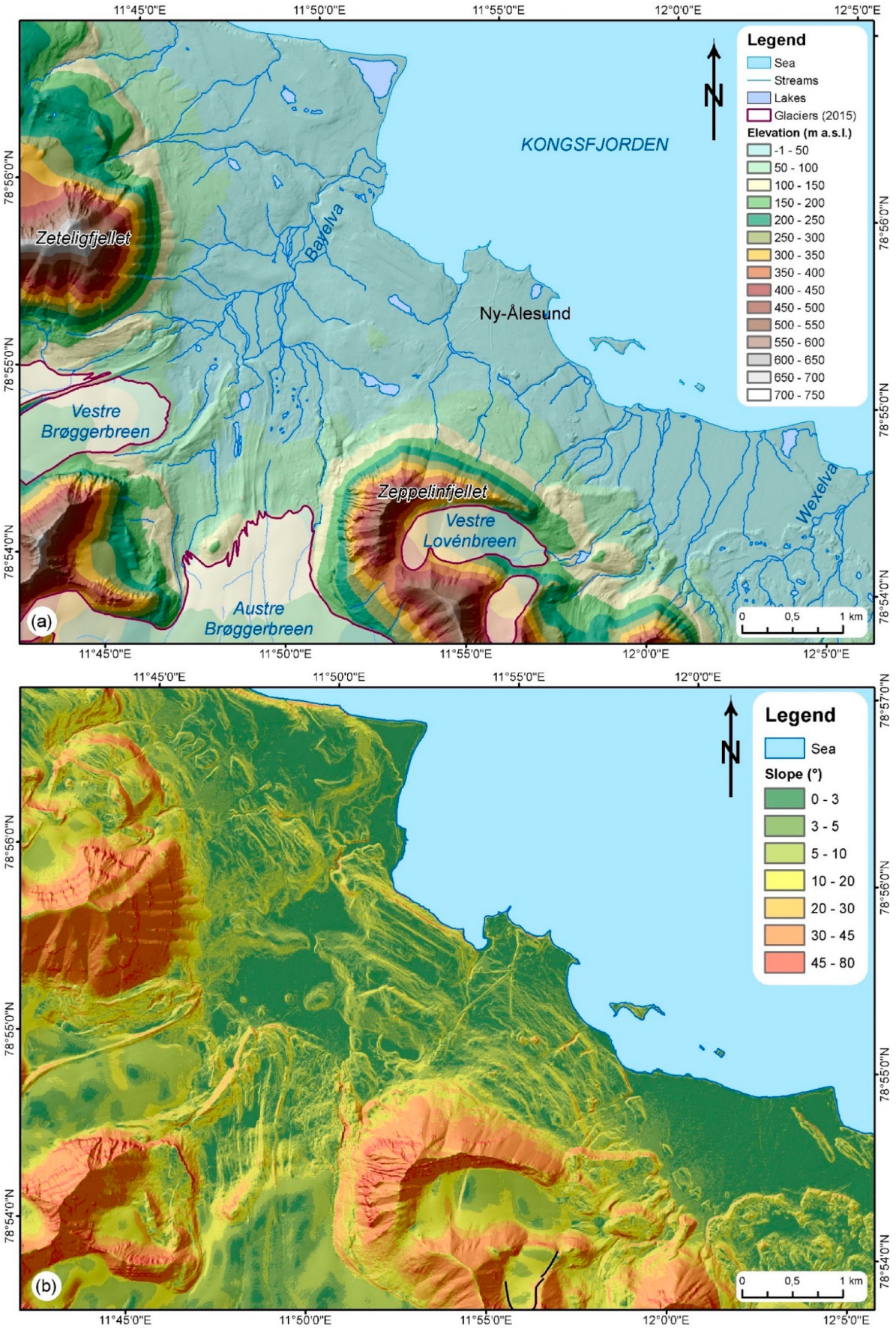

Figure 3. Orographic and hydrographic features of the Ny-Ålesund area (location in Figure 1); base data data from Norwegian Polan Institute (https://geodata.npolar.no/).. (a) Elevation distribution and hydrography; (b) Slope distribution.

NW side of the area, where the Bayelva river forms a large delta; Figure 4h) and rocky cliffs (in the airport and Ny-Ålesund area; Figure 4i). SE from Ny-Ålesund, a gravel beach is present (up to 100 m wide). Anthropogenic landforms and deposits are related to the intense coal mining that took place in the area from 1916 to 1963 and to the recent activities related to the international scientific stations in Ny-Ålesund.

4.2. Geomorphological map

The overall morphology of Blomstrandøya shows a large flat summit area (at 270–330 m a.s.l.), in which N-S are present. It is bounded by very steep (>45°) slopes along the NW and N sides and by gentle slopes (20–40°) in the S and SE flanks (Figure 5). The steep slopes are rimmed by strandflats at 10–90 m a.s.l. from 1.3 km (southern coast) to less than

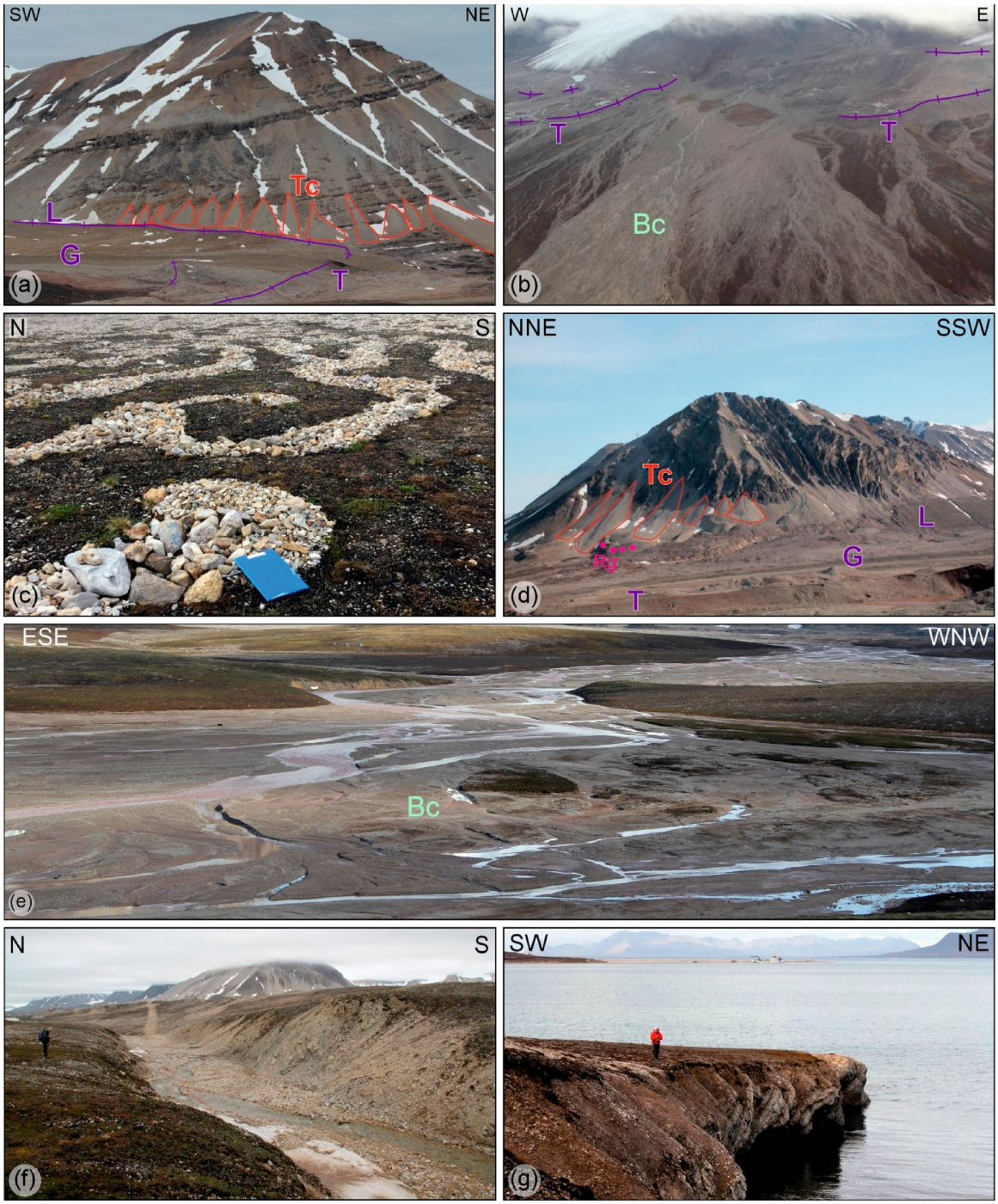

Figure 4. Quaternary deposits and landforms of the Ny-Ålesund area. (a) Terminal (T), lateral (L), and ground (G) moraines of Vestre Brøggerbreen; in the background talus cones (Tc) on the slope of Zeteligfjellet; (b) Terminal moraine (T) of the Vestre and Midtre Lovénbreen and braided channel (Bc) of the glacial outwash (Wexelva); (c) Periglacial patterned ground on the Bayelva area; (d) Talus cones (Tc) affecting the structural scarps and ridges on the slopes of Zeppelinfjellet, at the base of the slope a rock-glacier (Rg) and in the foreground the moraine (L, lateral; G, ground; T, terminal) system of the Austre Brøggerbreen; (e) Bayelva braided channel (Bc) and fluvial deposits in the Vestre Brøggerbreen and Austre Brøggerbreen glacier outwash; (f) Fluvial erosion scarps affecting the bedrock northern tributary of Bayelva; (g) Coastal cliff affecting the Kolhamna coast (airport area).

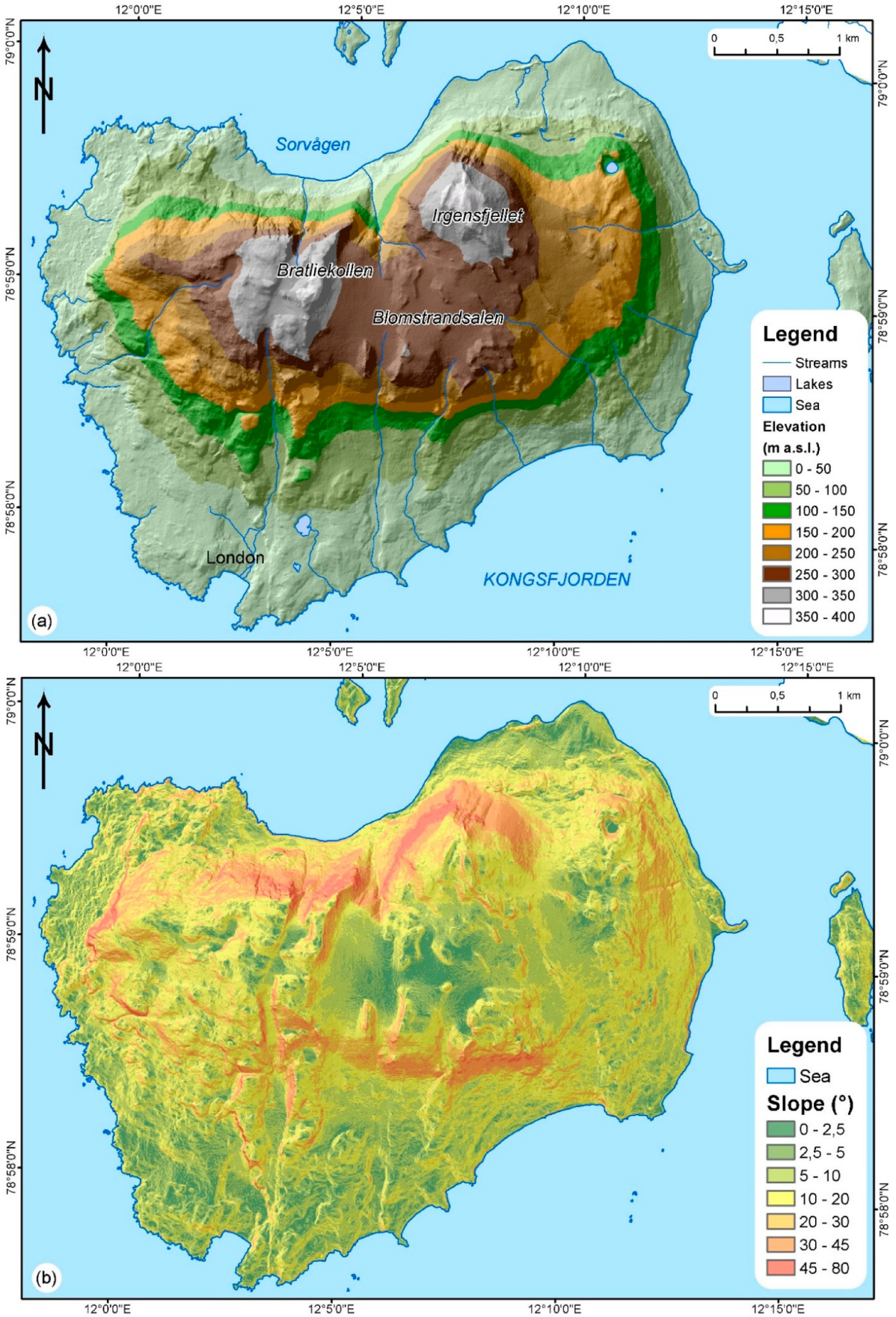

Figure 5. Orographic and hydrographic features of the Blomstrandøya area (location in Figure 1); base data from Norwegian Polan Institute (https://geodata.npolar.no/). (a) Elevation distribution and hydrography; (b) Slope distribution.

100 m wide (northern coast). The island has a ~20 km long coastline, 2/3 of which with a rocky shoreline with steep coastal cliffs (5–20 m high) and small pocket beaches; narrow beaches characterise the remaining 1/3 (mostly N and SW side). The W side of the island is mostly barren and rocky, while

surficial deposits cover the bedrock mainly on the E sides.

Surficial deposits are scattered and thin in the W part of the island; thin and widespread in the summit; and thicker and more continuous in the S part of the island as well as in the E and NE sector (Figure 6). A thick (up to >10–15 m) cover of recent (i.e. post-LIA) till and diamicton deposits is present in the northern coast, composing the terminal moraine of the Blomstrandbreen glacier originally connected to the island (Figure 6a). The diamicton deposits on the S, W-NW-facing slopes and are from moderately to heavily reworked by periglacial and fluvial processes. A large extent of reworked till deposit (thickness up to >10 m, derived from geomorphological correlation) is present over the flat summit area and along the eastern slope and is heavily affected by periglacial processes (Figure 6b).

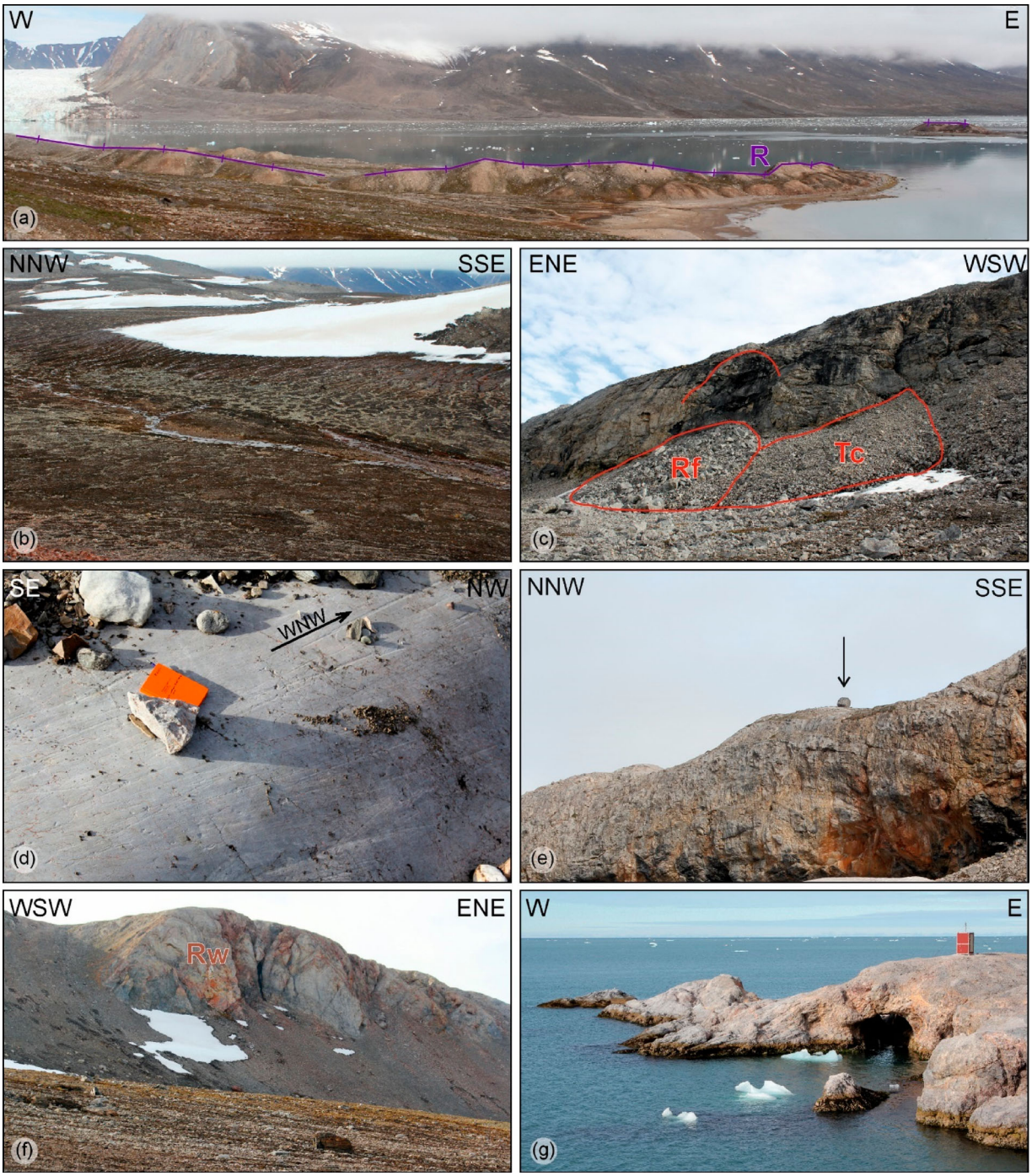

Figure 6. Quaternary deposits and landforms of the Blomstrandøya area. (a) Recessional moraine (R) related to the retreat of Blomstrandbreen in the NE side of the island (Burton et al. 2016); (b) Wide areas affected by periglacial patterned ground and solifluction evidences (on the flat summit area); (c) Rock fall (Rf)and talus cone (Tc) in the western scarp of the island; (d) *Roche moutonnée* on marble bedrock outlining W- to WNW-flow (SW side of the island); (e) Erratic boulder (arrow) on one of the top ridges of the island at ~170 m a.s.l.; (f) Steep rock wall on the side of the main ridges of the island (Bratliekollen, northern side of the island); (g) Coastal cliffs and caves affecting the marble rocks (western side of the island).

Along the N, NW, and S rock slopes of the island, large accumulations of talus slopes and cones and rockfall deposits are present (Figure 6c,f, and main map). At the base of steep-vertical rock scarps (NW side of the island), rockfall deposits are present. On the N side, these deposits are affected by periglacial processes (rock glaciers-protalus rampart).

Along the main N-S valleys, fluvial deposits result from the rework of glacial deposits into braided channels and alluvial fans.

Along the S and NW flatland surrounding the island, the bedrock is covered by beach deposits raised at elevations up to 37–40 m a.s.l. (see main map). Along the coast narrow and discontinuous gravel beach deposits are present.

4.2.1. Geomorphological features

Blomstrandøya preserves the evidence of ancient (LGM) glacial landforms. Small scale roches moutonnées are well preserved on the SW side of the island and testify to a W and WNW glacier flow (Figure 6d). Erratic boulders are scattered on the island up to the top of the summit ridges (Figure 6e), confirming that the island was entirely ice-covered at least during the LGM. Recent (post-LIA) glacial landforms are present on the NE side of the island. The moraine system of Blomstranbreen glacier features terminal and recessional moraines (according to Schomacker 2011; Figure 6a), from the LIA and more recent surges episodes, connected to submerged corresponding landforms (Burton et al. 2016; Hagen et al. 1993; Streuff 2013).

In many areas of the island, other processes largely overprint the glacial (LGM and LIA related) landforms. Periglacial features (i.e. patterned grounds and solifluction) mainly affect the till and diamicton reworked deposits on the flat summit area and along the slopes (Figure 6c). Slope landforms consist of rockfalls and talus slopes and cones, and protalus ramparts (Figure 6c,f, and main map). During the summer season, fluvial processes heavily rework glacial deposits forming braided channels, alluvial plains and fans. The rocky shoreline (W part of the island) features vertical cliffs on exposed bedrock with marine caves and pocket beaches (Figure 6g). On the E side, a long cliff has developed on bedrock covered by till and diamicton deposits. Along 1/3 of the coast, narrow gravel beaches are present. Moreover, flights of raised beaches can be found up to 37–40 m a.s.l. along the SW and NW strandflats (see main map).

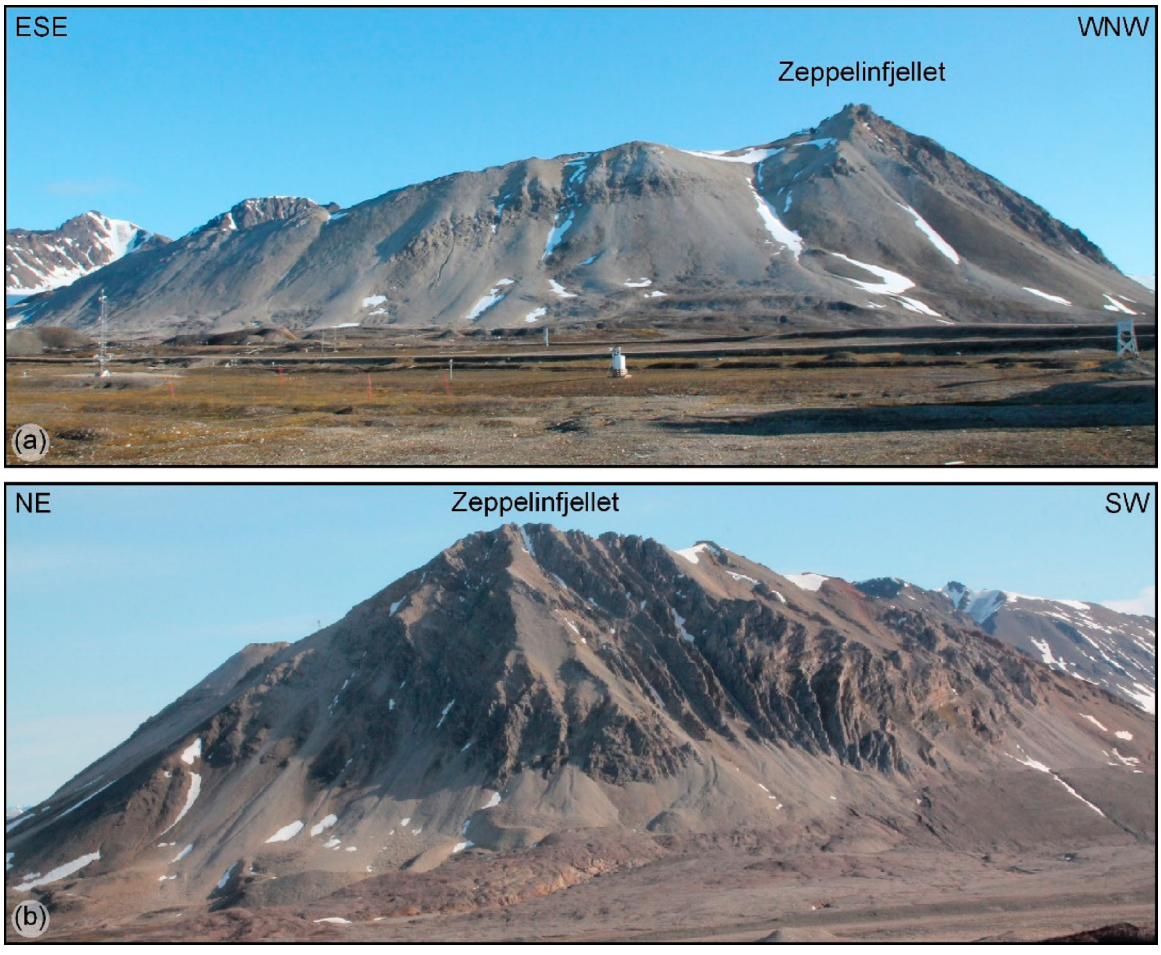

Figure 7. Panoramic view of the Zeppelinfjellet rock slope: (a) NE side, (b) NW side.

4.3. Fan-shaped landforms and talus slope distributions

The analysis of the fan-shaped landforms distribution (see De Haas et al. 2015 for a general review and Tomczyk and Ewertowski 2017, for geomorphological mapping in other areas of Svalbard) was focused in two specific areas: northern and western rock slopes of Zeppelinfjellet (south from Ny-Ålesund, Figure 7 and Figure 9a) and the rock slope of Bratliekollen-Irgensfjellet (northern slope of Blomstrandøya; Figures 8 and 9b).

The two sites are characterised by different types of fan-shaped landforms, including alluvial fans (debris-flows-dominated fans and fluvial-flow-dominated fans of Tomczyk and Ewertowski 2017) talus cones and wider talus slopes (colluvial fan of Tomczyk and Ewertowski 2017), the latter mostly affected by gravitational mass movements (Figures 7 and 8).

In the Zeppelinfjellet slope (Ny-Ålesund), the total volume of the slope deposits was estimated as 1,216,200 m^3. The total extent of the source areas of the sediments is 578,700 m^2 for an average eroded thickness of 2.10 m. In the Bratliekollen slope (Blomstrandøya), the total volume of the slope deposits was estimated as 1,611,600 m^3. The total extent of the source areas of the sediments on the rock walls is 564,600 m^2 for an average eroded thickness of 2.85 m. The calculated average erosion is underestimated since part of the material is removed by runoff and erosional processes. This calculation does not take into account and assume as zero the removed material. This assumption is consistent with the geomorphological conditions, which outline low erosional processes at the base of the studied slope (only minor tributary channels in unglaciated areas), with erosion rates in the order of ~0.015–0.040 mm/yr (Bogen and Bønsnes 2003; 1996; Svendsen, Mangerud, and Miller 1989).

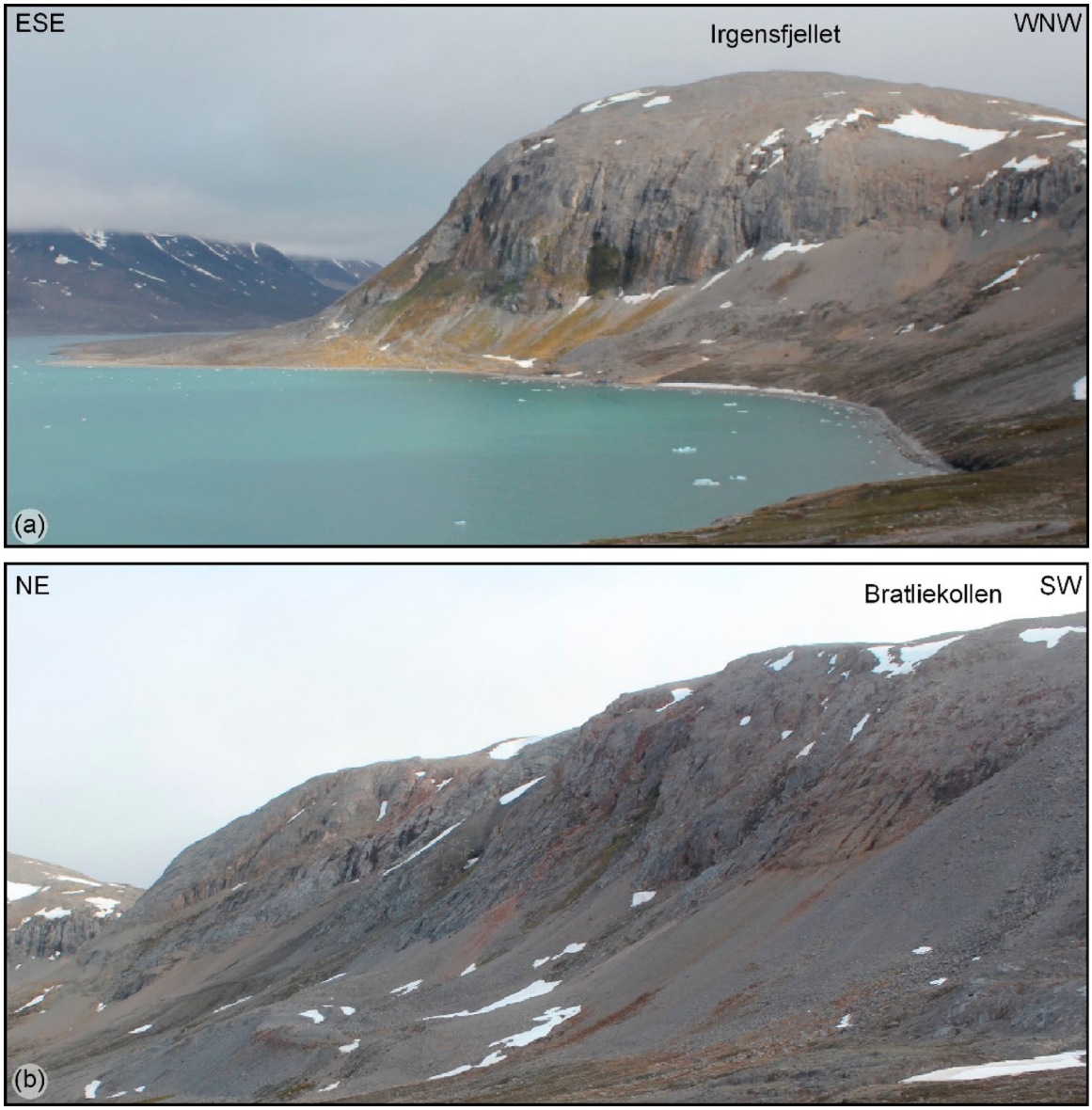

Figure 8. Panoramic view of the Irgensfjellet (a) and Bratliekollen (b) rock slopes.

Considering these limitations and the assumption, we tried to derive the expected rates of erosion along the slopes and rock walls due to gravity-driven processes, or at least a minimum possible rate. According to Henriksen et al. (2014), the Kongsfjorden glacier retreated from the fjord form 14 kyrs to 11 kyrs. This means that at this time the rock slopes of Zeppelinfjellet and Bratliekollen were most likely ice-free and affected by slope processes. Assuming that the fan-shaped landforms and talus slopes started forming at that time, the average rate of erosion of the rock slopes over the Holocene period is 0.15–0.19 mm/yr

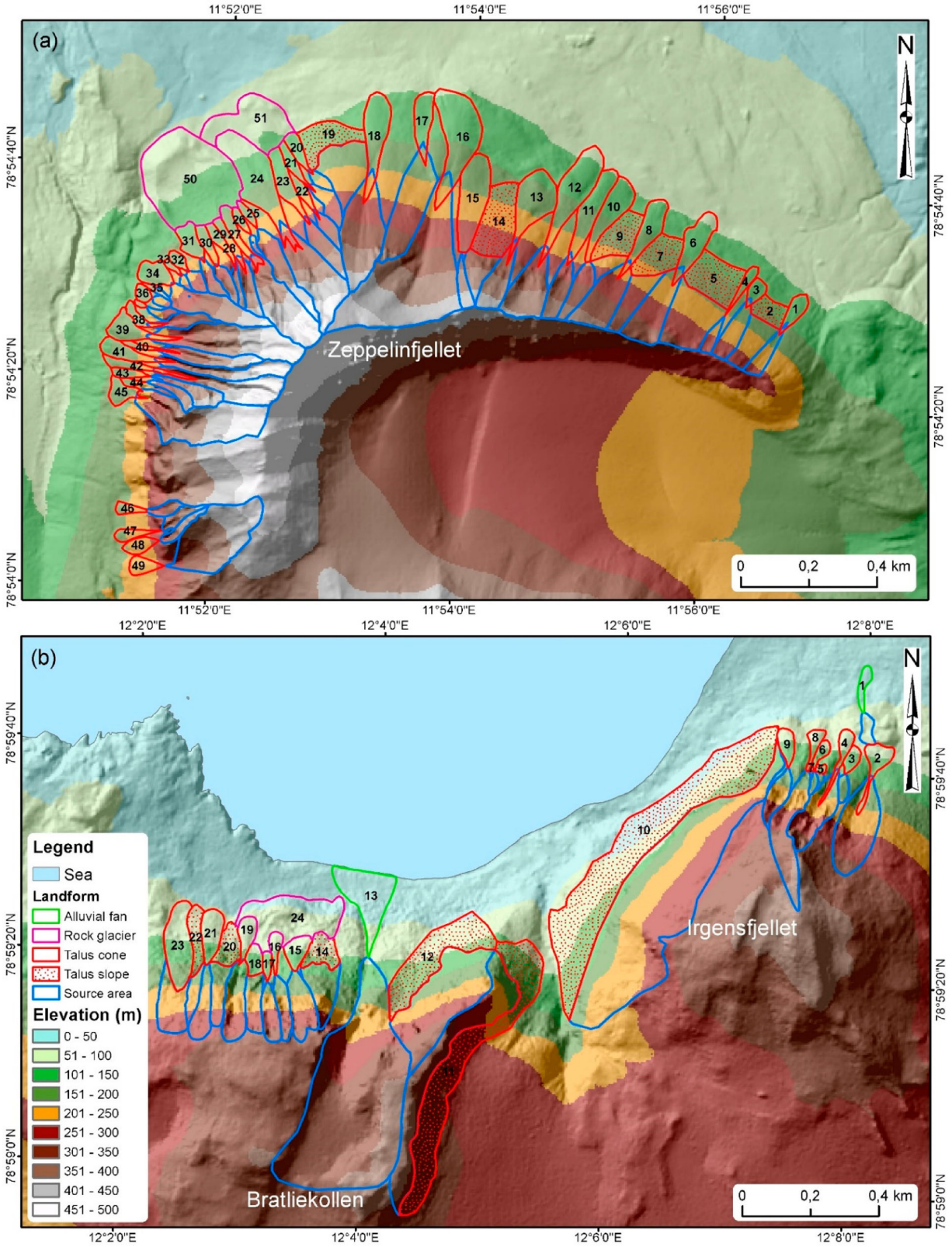

Figure 9. Fan-shaped landforms and talus slopes distribution on (a) Zeppelinfjellet slope (Ny-Ålesund) and (b) Bratliekollen slope (Blomstrandøya); the numbers refer to Tables 2 and 3.

for the Zeppelinfjellet slope and 0.20–0.25 mm/yr for the Bratliekollen slope.

If we include in the calculation the landforms such as rock glaciers and protalus rampart, which indeed rework slope deposits (Berthling and Etzelmüller 2007), both in Zeppelinfjellet and Bratliekollen, the estimated eroded volumes are largely higher. In the Zeppelinfjellet slope, due to two landforms with a total surface extent of ~87,600 m^2 and an average thickness of ~30 and 15 m, the additional volume is 1,119,750 m^3 (estimating a ~50% of ice volume in the rock glaciers), and the total volume of eroded sediments is 2,335,950 m^3. This means an average eroded thickness of 4.04 m. Consequently, the average rate of erosion over the Holocene period increases to 0.29–0.37 mm/yr. In the Bratliekollen slope, a landform with a surface extent of ~49,000 m^2 and an average thickness of ~20 m is present. The additional volume is 490,000 m (again estimating a ~50% of ice volume)[3], and the total volume of eroded sediments is 2,101,600 m^3. The average eroded thickness reaches the value of 3.72 m, and the rate of erosion over the Holocene period increases to 0.27–0.34 mm/yr. The underestimation of these values due to the sediment transfer and removal from the fan-shaped landforms can be roughly 4–8% (~0.011–0.029 mm/yr over 0.27–0.37 mm/yr).

Table 2. Fan-shaped landforms and talus slopes on (a) Zeppelinfjellet slope (Ny-Ålesund).

Id	Type	Area (m^2)	Extimated Thickness (m)	Extimated volume (m^3)	Source Area (m^2)
1	Talus cone	4365	3	13095	5386
2	Talus slope	6400	2	12800	11062
3	Talus cone	3089	2	6178	8754
4	Talus cone	2692	3	8076	3066
5	Talus slope	17725	3	53175	23878
6	Talus cone	10890	5	54450	18799
7	Talus slope	12722	3	38166	10784
8	Talus cone	10217	5	51085	18190
9	Talus slope	12689	3	38067	4423
10	Talus cone	12169	4	48676	8147
11	Talus cone	13203	5	66015	9164
12	Talus cone	20136	5	100680	18230
13	Talus cone	16861	10	168610	11226
14	Talus slope	20691	4	82764	8352
15	Talus cone	19460	4	77840	4362
16	Talus cone	26834	15	402510	81273
17	Talus cone	8148	5	40740	27018
18	Talus cone	14675	8	117400	30337
19	Talus slope	13565	3	40695	19423
20	Talus cone	3852	5	19260	2362
21	Talus cone	3545	5	17725	5919
22	Talus cone	3001	5	15005	4059
23	Talus cone	8461	6	50766	8252
24	Talus cone	27367	15	410505	27147
25	Talus cone	1850	5	9250	12323
26	Talus cone	1867	5	9335	1023
27	Talus cone	5309	5	26545	25734
28	Talus cone	3574	4	14296	6669
29	Talus cone	3193	4	12772	2312
30	Talus cone	3489	30	104670	3999
31	Talus cone	5518	6	33108	4067
32	Talus cone	2033	8	16264	2851
33	Talus cone	1003	5	5015	1036
34	Talus cone	5931	10	59310	17738
35	Talus cone	480	5	2400	667
36	Talus cone	1924	7	13468	1359
37	Talus cone	518	5	2590	2148
38	Talus cone	2740	5	13700	5570
39	Talus cone	8007	18	144126	33248
40	Talus cone	1593	4	6372	10599
41	Talus cone	6388	10	63880	13506
42	Talus cone	4194	5	20970	19200
43	Talus cone	2403	4	9612	7073
44	Talus cone	1061	4	4244	3834
45	Talus cone	4657	7	32599	38547
46	Talus cone	2101	5	10505	2921
47	Talus cone	2702	5	13510	3837
48	Talus cone	3452	5	17260	3549
49	Talus cone	3538	5	17690	36264
50	Rock glacier – pr. rampart	61,700	30	1,851,000	
51	Rock glacier – pr. rampart	25,900	15	388,500	

Table 3. Fan-shaped landforms and talus slopes on Bratliekollen slope (Blomstrandøya).

Id	Type	Area (m^2)	Extimated Thickness (m)	Extimated volume (m^3)	Source Area (m^2)
1	Alluvial fan	2,922	5	14,610	3,009
2	Talus cone	6,317	6	37,902	25,984
3	Talus cone	2,643	3	7,929	2,205
4	Talus cone	4,060	5	20,300	16,652
5	Talus slope	716	4	2,864	762
6	Talus cone	2,098	3	6,294	1,169
7	Talus slope	216	3	648	179
8	Talus cone	2,913	4	11,652	20,617
9	Talus cone	3,966	6	23,796	7,161
10	Talus slope	10,8367	15	1,625,505	145,303
11	Talus slope	60,051	10	600,510	46,832
12	Talus slope	32,356	10	323,560	50,467
13	Alluvial fan	21,275	5	106,375	152,665
14	Talus slope	7,632	5	38,160	12,680
15	Talus cone	5,155	8	41,240	12,193
16	Talus cone	2,812	5	14,060	6,446
17	Talus cone	1,840	4	7,360	7,388
18	Talus cone	3,829	3	11,487	8,184
19	Talus cone	4,803	6	28,818	13,457
20	Talus slope	7,016	5	35,080	8,154
21	Talus cone	7,916	8	63,328	8,789
22	Talus slope	6,716	5	33,580	4,654
23	Talus cone	16,417	8	131,336	12,759
24	Talus slope	14,197	3	42,591	
25	Rock glacier – pr. rampart	49,000	20	980,000	

5. Conclusions

The geomorphological analysis carried out in the Kongsfjorden area, integrating field and remote investigations, yielded: (1) the geomorphological maps of Ny-Ålesund area and the Blomstrandøya, and (2) a specific analysis of the slope processes along rock slopes.

The geomorphological maps led to the comprehension of the distribution of landforms in different paraglacial environments from recently deglaciated areas, after the LIA (1800–2000; i.e. Austre and Vestre Brøggerbreen glacier front and Bayelva, Ny-Ålesund; northern Blomstrandøya) to ancient deglaciated areas, after LGM (Late Pleistocene-Early Holocene; i.e. the entire Blomstrandøya, the Ny-Ålesund strandflat and rock slopes). The main terrestrial glaciers are present-day remnants of the massive, composite,

W-NW flowing, valley glacier that occupied Kongsfjorden during the LGM. At that time, the entire fjord was ice-filled up to the top of Blomstrandøya, which can be considered as a large scale roches moutonnées and whose overall shape (gentle E-SE slopes; steep NW escarpments) and locally preserved roches moutonnées confirm a W-NW flow. They have been retreating from the main valleys with alternating stages of ice advance and surges (e.g. LIA and in the last century, Burton et al. 2016; Hagen et al. 1993; Hormes, Gjermundsen, and Rasmussen 2013 and references therein). The ancient glacial landforms are overprinted by periglacial (i.e. patterned ground), fluvial (i.e. alluvial plains and braided channels), and slope landforms (i.e. talus cones and slopes). In the Blomstrandøya SW strandflat, remnants of a sequence of raised beaches are preserved up to 37–40 m a.s.l., whose uplift is related to the postglacial retreat isostatic rebound, confirming the sequence of raised beaches well documented in the Brøggeralvøya NW termination (e.g. by Forman 1990; Forman, Mann, and Miller 1987). A strong glacier retreat occurred over the last decades and was calculated as high as ~30 m/yr from 1998 to 2015 (in Austre-Vestre Brøggerbreen), and is consistent with the previous calculations (e.g. Burton et al. 2016; Gjermundsen et al. 2013; Hagen et al. 1993; Svendsen et al. 2002).

Finally, the analysis of the rock slopes and related deposits of Zeppelinfjellet (Ny-Ålesund) and Bratliekollen (Blomstrandøya) allowed to infer the average rate of erosion over the Holocene. Assuming that the slopes were ice-free and affected by slope processes from 14 kyrs to 11 kyrs (according to Henriksen et al. 2014), the estimated erosion rate is 0.15–0.19 mm/yr for the Zeppelinfjellet slope and 0.20–0.25 mm/yr for the Bratliekollen slope. Including into the calculation the periglacial slope landforms, the average rate of erosion over the Holocene raises to 0.29–0.37 mm/yr, in the Zeppelinfjellet slope, and 0.27–0.34 mm/yr, in the Bratliekollen slope (with an underestimation of ~4–8%). These estimated erosion rates along the rock walls are very high taking into account that different strong lithologies are considered (i.e. conglomerate, sandstone and shale with limestone, dolomite in the Zeppelinfjellet slope; marbles in Bratliekollen slope). However, the values are largely consistent with the rock walls erosion rates connected with postglacial relaxation processes (André 1997), as found in the Prins Karls Forland, just offshore the Kongsforden (i.e. 0.13–0.64 mm/yr, Berthling and Etzelmüller 2007). They are even close to the highest rock wall erosion rates measured in arctic environments (Siewert et al. 2012) and can also be affected by rock permafrost changes.

This study confirms geomorphological mapping integrating field and remote investigations as an effective tool, particularly at high latitudes in poorly vegetated terrains, in the comprehension of landscape changes in the paraglacial environment. For this reason, in this case, a specific analysis was focused on the slope gravity-driven landforms, which record the effects of deglaciation on the main mountain slopes. This allows the identification of post-deglaciation slope evolution and provides a comparison to rock slopes in other present or past mountain and cold environments.

Software

The map presented in this work was produced in the Geographic Information System ArcGIS® 10.6.1 (ESRI).

Acknowledgments

The authors wish to thank the Reviewers Aleksandra Tomczyk, Denis Mercier, and Chris Orton, as well as the Associated Editor Jasper Knight, whose preciuìous suggestions and comments helped us to improve the map and manuscript. The authors are grateful to CNR-Italy for supporting this research activity, particularly the Department of Earth System Science and Environmental Technologies, the Polarnet, and the Institute of environmental geology and geoengineering (IGAG). Special thanks also go also to the 'Dirigibile Italia' Station, CNR-Italy (particularly to R. Sparapani and E. Liberatori) for the outstanding logistic support during all the field work. A great support was provided also by Christiane Hübner (SSF) and by Kings Bay AS. The authors are particularly grateful for the fruitful discussion with A. Hormes and H. Linge, Project HolS, Holocene environmental change on Svalbard (RIS 5842). This work was carried out as part of the RIS 10150 project (http://www.researchinsvalbard.no/). The digital elevation models, aerial images and orthophotos used in this work where provided by the Norwegian Polar Institute.

Disclosure statement

No potential conflict of interest was reported by the author (s).

Funding

This work was supported by the Norwegian Research Council (SSG 2016 grant, SLOPES project RIS 10150, P.I. I.T. Berthling) and by the 'G. d'Annunzio' Chieti Pescara funds (E. Miccadei funds).

ORCID

Ivar T. Berthling http://orcid.org/0000-0003-0003-1651
Claudio Berti http://orcid.org/0000-0001-6453-2645
Vania Mancinelli http://orcid.org/0000-0001-6594-828X
Laura Stendardi http://orcid.org/0000-0002-9802-8962
Tommaso Piacentini http://orcid.org/0000-0002-5007-7677
Enrico Miccadei http://orcid.org/0000-0003-2114-2940

References

André, M. F. (1997). Holocene rockwall retreat in Svalbard: A triple-rate evolution. *Earth Surface Processes and Landforms*, *22*(5), 423–440. https://doi.org/10.1002/(SICI)1096-9837(199705)22:5<423::AID-ESP706>3.0.CO;2-6

André, M. F. (2009). From climatic to global change geomorphology: Contemporary shifts in periglacial geomorphology. *Geological Society Special Publication*, *320*(1), 5–28. https://doi.org/10.1144/SP320.2

Ballantyne, C. K. (2002). Paraglacial geomorphology. *Quaternary Science Reviews*, *21*(18-19), 1935–2017. https://doi.org/10.1016/S0277-3791(02)00005-7

Bergh, S., Maher, H., & Braathen, A. (2000). Tertiary divergent thrust directions from partitioned transpression, Brøggerhalvøya, Spitsbergen. *Norsk Geologisk Tidsskrift*, *80*(2), 63–81. https://doi.org/10.1080/002919600750042573

Bernard, E., Friedt, J. M., Schiavone, S., Tolle, F., & Griselin, M. (2018). Assessment of periglacial response to increased runoff: An Arctic hydrosystem bears witness. *Land Degradation & Development*, *29*(10), 3709–3720. https://doi.org/10.1002/ldr.3099

Berthling, I. T., & Etzelmüller, B. (2007). Holocene rockwall retreat and the estimation of rock glacier age, Prins Karls Forland, Svalbard. *Geografiska Annaler, Series A: Physical Geography*, *89*(1), 83–93. https://doi.org/10.1111/j.1468-0459.2007.00309.x

Bogen, J., & Bønsnes, T. E. (2003). Erosion and sediment transport in High Arctic rivers. *Svalbard Polar Research*, *22*(2), 175–189. https://doi.org/10.3402/polar.v22i2.6454

Boike, J, Juszak, I, Lange, S, Chadburn, S, Burke, E, Paul Overduin, P, Roth, K, Ippisch, O, Bornemann, N, Stern, L, Gouttevin, I, Hauber, E, & Westermann, S. (2018). A 20-year record (1998-2017) of permafrost, active layer and meteorological conditions at a high Arctic permafrost research site (Bayelva, Spitsbergen). *Earth System Science Data*, *10*(1), 355–390.

Bourriquen, M., Mercier, D., Baltzer, A., Fournier, J., Costa, S., & Roussel, E. (2018). Paraglacial coasts responses to glacier retreat and associated shifts in river floodplains over decadal timescales (1966–2016), Kongsfjorden, Svalbard. *Land Degradation & Development*, *29*(11), 4173–4185. https://doi.org/10.1002/ldr.3149

Burton, D. J., Dowdeswell, J. A., Hogan, K. A., & Noormets, R. (2016). Marginal fluctuations of a Svalbard surge-type tidewater glacier, Blomstrandbreen, since the Little Ice Age: A record of three surges. *Arctic, Antarctic, and Alpine Research*, *48*(2), 411–426. https://doi.org/10.1657/AAAR0014-094

Church, M., & Ryder, J. M. (1972). Paraglacial sedimentation: Consideration of fluvial processes conditioned by glaciation. *Geological Society of America Bulletin*, *83*(10), 3059–3072. https://doi.org/10.1130/0016-7606(1972)83[3059:PSACOF]2.0.CO;2

Cianfarra, P., & Salvini, F. (2015). Lineament domain of regional strike-slip corridor: Insight from the neogene transtensional de geer transform fault in NW spitsbergen. *Pure and Applied Geophysics*, *172*(5), 1185–1201. https://doi.org/10.1007/s00024-014-0869-9

Cianfarra, P., & Salvini, F. (2016). Quantification of fracturing within fault damage zones affecting Late Proterozoic carbonates in Svalbard. *Rendiconti Lincei*, *27*(S1), 229–241. https://doi.org/10.1007/s12210-016-0527-5

De Haas, T., Kleinhans, M. G., Carbonneau, P. E., Rubensdotter, L., & Hauber, E. (2015). Surface morphology of fans in the high-Arctic periglacial environment of Svalbard: Controls and processes. *Earth Science Reviews*, *146*, 163–182. https://doi.org/10.1016/j.earscirev.2015.04.004

Esri, Maxar, Earthstar Geographics. (2015). CNES/Airbus DS, USDA FSA, USGS, Aerogrid, IGN, IGP, and the GIS User Community (Date 2015-07-15; Resolution 0,50 m; Accuracy 10,20 m; Data Source WV02.

Etienne, S., Mercier, D., & Voldoire, O. (2008). Temporal scales and deglaciation rhythms in a polar glacier margin, Baronbreen, Svalbard. *Norsk Geografisk Tidsskrift – Norwegian Journal of Geography*, *62*(2), 102–114. https://doi.org/10.1080/00291950802095111

Etzelmüller, B., Ødegard, R. S., & Sollid, J. L. (2003). *The spatial distribution of coast types on Svalbard*. In V. Rachold et al (Eds.), *Arctic coastal Dynamics: Report of the 3rd international Workshop University of Oslo (Norway) 25 December 2002* (pp. 33–40). Berichte zur Polarforschung und Meereforschung 443.

Evans, D. J. A., Strzelecki, M., Milledge, D. G., & Orton, C. (2012). Hørbyebreen polythermal glacial landsystem, Svalbard. *Journal of Maps*, *8*(2), 146–156. https://doi.org/10.1080/17445647.2012.680776

Forman, S. L. (1990). Post-glacial relative sea-level history of northwestern Spitsbergen, Svalbard. *Geological Society of America Bulletin*, *102*(11), 1580–1590. https://doi.org/10.1130/0016-7606(1990)102<1580:PGRSLH>2.3.CO;2

Forman, S. L., Lubinski, D. J., Ingolfsson, O., Zeeberg, J. J., Snyder, J. A., Siegert, M. J., & Matishov, G. G. (2004). A review of postglacial emergence on Svalbard, Franz Josef Land and Novaya Zemlya, northern Eurasia. *Quaternary Science Reviews*, *23*(11-13), 1391–1434. https://doi.org/10.1016/j.quascirev.2003.12.007

Forman, S., Mann, D., & Miller, G. (1987). Late Weichselian and Holocene relative sea-level history of Bröggerhalvöya, Spitsbergen. *Quaternary Research*, *27*(1), 41–50. https://doi.org/10.1016/0033-5894(87)90048-2

Gjermundsen, E. F., Briner, J. P., Akçar, N., Salvigsen, O., Kubik, P., Gantert, N., & Hormes, A. (2013). Late Weichselian local ice dome configuration and chronology in Northwestern Svalbard: Early thinning, late retreat. *Quaternary Science Reviews*, *72*, 112–127. https://doi.org/10.1016/j.quascirev.2013.04.006

Hagen, J., Liestøl, O., Roland, E., & Jørgensen, T. (1993). Glacier atlas of Svalbard and Jan Mayen. *Nor. Polarinst. Medd*, *129*, 141 pp.

Hallet, B. (2013). Stone circles: Form and soil kinematics. *Philosophical Transactions of the Royal Society A: Mathematical, Physical and Engineering Sciences*, *371*(2004), 20120357. https://doi.org/10.1098/rsta.2012.0357

Hallet, B., & Prestrud, S. (1986). Dynamics of periglacial sorted circles in Western Spitsbergen. *Quaternary Research*, *26*(1), 81–99. https://doi.org/10.1016/0033-5894(86)90085-2

Hasholt, B. (1996). Sediment transport in Greenland. *IAHS-AISH Publication*, *236*, 105–114.

Henriksen, M., Alexanderson, H., Landvik, J. Y., Linge, H., & Peterson, G. (2014). Dynamics and retreat of the Late Weichselian Kongsfjorden ice stream, NW Svalbard. *Quaternary Science Reviews*, *92*, 235–245. https://doi.org/10.1016/j.quascirev.2013.10.035

Hjelle, A. (1993). *Geology of Svalbard. Polarha°ndbok 7*. Norwegian Polar Institute.

Hjelle, A., Piepjohn, K., Saalmann, K., Ohta, Y., Salvigsen, O., Thiedig, F., & Dallmann, W. (1999). Geological map of Svalbard 1:100.000 Sheet A7G Kongsfjorden. *Norvegian Polar Institute*, *30*.

Hormes, A., Gjermundsen, E. F., & Rasmussen, T. L. (2013). From mountain top to the deep sea - deglaciation in 4D of the northwestern Barents Sea. *Quaternary Science Reviews*, *75*, 78–99. https://doi.org/10.1016/j.quascirev.2013.04.009

Humlum, O., Instanes, A., & Sollid, J. L. (2003). Permafrost in Svalbard: A review of research history, climatic background and engineering challenges. *Polar Research*, *22* (2), 191–215. https://doi.org/10.3402/polar.v22i2.6455

Joly, P. F. (1969). *Carte Géomorphologique de reconnaissance de la presqu'île de Brögger (Spitsberg)*. 1:50.000. Service de documentation et de cartographie géographiques du C.N.R.S. Institut du Géographie. Paris.

Kääb, A., Ramuntcho Girod, L. M., & Berthling, I. T. (2014). Surface kinematics of periglacial sorted circles using structure-from-motion technology. *The Cryosphere*, *8* (3), 1041–1056. https://doi.org/10.5194/tc-8-1041-2014

Laffly, D., & Mercier, D. (2002). Global change and paraglacial morphodynamic modification in Svalbard. *International Journal of Remote Sensing*, *23*(21), 4743–4760. https://doi.org/10.1080/01431160110113872

Leever, K. A., Gabrielsen, R. H., Faleide, J. I., & Braathen, A. (2011). A transpressional origin for the West Spitsbergen fold-and-thrust belt: Insight from analog modelling. *Tectonics*, *30*, TC2014. https://doi.org/10.1029/2010TC002753

Lehmann, S. J., & Forman, S. L. (1992). Late Weichselian Glacier Retreat in Kongsfjorden, West Spitsbergen, Svalbard. *Quaternary Research*, *37*(2), 139–154. https://doi.org/10.1016/0033-5894(92)90078-W

Mercier, D., Étienne, S., Sellier, D., & André, M. F. (2009). Paraglacial gullying of sediment-mantled slopes: A case study of Colletthøgda, Kongsfjorden area, west Spitsbergen (Svalbard). *Earth Surface Processes and Landforms*, *34*(13), 1772–1789. https://doi.org/10.1002/esp.1862

Mercier, D., & Laffly, D. (2005). *Actual paraglacial progradation of the coastal zone in the Kongsfjorden area, West Spitsbergen (Svalbard)*. In C. Harris, & J. Murton (Eds.), *Cryospheric systems: Glaciers and permafrost, Special Publication, 242* (pp. 111–117). Geological Society. https://doi.org/10.1144/GSL.SP.2005.242.01.10

Miccadei, E., Piacentini, T., & Berti, C. (2016). Geomorphological features of the Kongsfjorden area: Ny-Ålesund, Blomstrandøya (NW Svalbard, Norway). Special Issue on environmental changes in the Arctic. *Rend. Fis. Acc. Lincei*, *27*(S1), 217–228. https://doi.org/10.1007/s12210-016-0537-3

Moreau, M., Mercier, D., Laffly, D., & Roussel, E. (2008). Impacts of recent paraglacial dynamics on plant colonization: A case study on midtre Lovénbreen foreland, Spitsbergen (79°N). *Geomorphology*, *95*(1-2), 48–60. https://doi.org/10.1016/j.geomorph.2006.07.031

Oliva, M., Mercier, D., Ruiz-Fernández, J., & McColl, S. (2019). Paraglacial processes in recently deglaciated environments. *Land Degradation & Development*, 1–6. https://doi.org/10.1002/ldr.3283

Pekala, K. (2004). *Geomorphological mapping, Wedel Jarlsberg Land, Svalbard, Version 1*. NSIDC: National Snow and Ice Data Center.

Rubensdotter, L., Larsen, E., & Lysså, A. (2016). *Quaternary geological and geomorphological map, Svea, Svalbard*. M 1:15.000. Geological Survey of Norway. https://www.ngu.no/upload/Publikasjoner/Kart/Svalbard/KV15_Svea_Svalbard.pdf

Rubensdotter, L., Stalsberg, K., Christiansen, H., Eckerstorfer, M., & Trøyen, P. (2015). *Landforms and sediments in Todalen and upper Gangdalen and Bødalen, Svalbard*. Scale 1:25 000. Geological Survey of Norway. http://www.ngu.no/upload/Publikasjoner/Kart/Svalbard/kart_todalen_engelsk.pdf

Schomacker, A. (2011). Moraine. In V. P. Singh, P. Singh, & Haritashya (Eds.), *U.K. encyclopedia of snow, ice and glaciers* (pp. 747–756). Springer.

Sessford, E., & Hormes, A. (2013). Quaternary geological and geomorphological maps of Fredheim and Scansbukta. *Norwegian Polar Institute Report*, Serie 142.

Siewert, M. B., Krautblatter, M., Christiansen, H. H., & Eckerstorfer, M. (2012). Arctic rockwall retreat rates estimated using laboratory-calibrated ERT measurements of talus cones in Longyeardalen, Svalbard. *Earth Surface Processes and Landforms*, *37*(14), 1542–1555. https://doi.org/10.1002/esp.3297

Slaymaker, O. (2009). *Proglacial, periglacial or paraglacial?* In J. Knight, & S. Harrison (Eds.), *Periglacial and paraglacial processes and environments, Special Publication 320* (pp. 71–84). The Geological Society.

Slaymaker, O. (2011). Criteria to distinguish between periglacial, proglacial and paraglacial environments. *Quaestiones Geographicae*, *30*(1), 85–94. https://doi.org/10.2478/v10117-011-0008-y

Streuff, K. (2013). *Landform assemblages in inner Kongsfjorden, Svalbard: Evidence of recent glacial (surge) activity* [Master thesis] Faculty of Science and Technology Department of Geology, University of Tromso.

Strzelecki, M. C., Szczuciński, W., Dominiczak, A., Zagórski, P., Dudek, J., & Knight, J. (2020). New fjords, new coasts, new landscapes: The geomorphology of paraglacial coasts formed after recent glacier retreat in Brepollen (Hornsund, southern Svalbard). *Earth Surface Processes and Landforms*, *45*(5), 1325–1334. https://doi.org/10.1002/esp.4819

Sund, M., & Eiken, T. (2010). Recent surges on Blomstrandbreen, Comfortlessbreen and Nathorstbreen, Svalbard. *Journal of Glaciology*, *56*(195), 182–184. https://doi.org/10.3189/002214310791190910

Svendsen, H., Beszczynska-Møller, A., Hagen, J. O., Lefauconnier, B., Tverberg, V., Gerland, S., … Dallmann, W. (2002). The physical environment of Kongsfjorden–Krossfjorden, an Arctic fjord system in Svalbard. *Polar Research*, *21*, 133–166. https://doi.org/10.1111/j.1751-8369.2002.tb00072.x

Svendsen, J. I., Mangerud, J., & Miller, G. H. (1989). Denudation rates in the Arctic estimated from lake sediments on Spitsbergen, Svalbard. *Palaeogeography, Palaeoclimatology, Palaeoecology*, *76*(1–2), 153–168. https://doi.org/10.1016/0031-0182(89)90108-9

Thiedig, F., & Manby, M. (1992). Origins and deformation of post-Caledonian sediments on Blomstrandhalvøya and Lovenøyane, northwest Spitsbergen. *Norsk Geologisk Tidsskrift*, *72*, 27–33.

Tolgensbakk, J., & Sollid, J. L. (1987). *Kvadehuksletta, geomorfologi og kvartaergeologi, 1:10.000*. Geografisk Institutt i Oslo.

Tolgensbakk, J., Sørbel, L., & Høgvard, K. (2001). *Geomorphological and Quaternary geological map of Svalbard 1:100,000, sheet C9Q Adventdalen*. Norvegian Polar Institute.

Tomczyk, A. M., & Ewertowski, M. W. (2017). Surface morphological types and spatial distribution of fan-shaped landforms in the periglacial high-Arctic environment of central Spitsbergen, Svalbard. *Journal of Maps*, *13* (2), 239–251. https://doi.org/10.1080/17445647.2017.1294543